

# Multicomponent inverse scattering series internal multiple prediction Part I: Analytical analysis of input preparation

Jian Sun\*, Kris Innanen\*, Daniel Trad\*, Yu Geng\*

## ABSTRACT

To date, most of presented approaches of internal multiples prediction or elimination assume an acoustic background model. In practice, the acoustic approximation will result in a false, misleading and potentially injurious estimate due to the neglect of the wave-mode conversion. The closer the reference model is to reality, the more accurate achieved prediction algorithm will be. Inverse scattering series has been revealed in extremely powerful capabilities of seismic data processing and inversion, such as full waveform inversion (FWI), direct non-linear AVO analysis, and surface-related or internal multiples attenuation on acoustic cases, due to its property of model independence. The 3D formulation of elastic internal multiples prediction algorithm was introduced by considering an isotropic-elastic-homogeneous reference medium, which evaluates the wave-mode conversion and multiples prediction in a self-acting manner. The input preparation is the essential step for the prediction. Since the wave-mode conversion can only be handled in the top layer, an inappropriate will misleads the conversion in lower layers which disorders lower-higher-lower relationship of events reflected by the same layer but with different wave mode conversions. In this paper, we analyse the possible input preparation methods for the algorithm implementing in different domains using wavenumber related elastic stolt migration, slowness related elastic stolt migration, time-stretching method in plane wave domain, and the best-fitting method with high resolution hyperbolic radon transform. The advantages and weaknesses of each approach are discussed.

## INTRODUCTION

In seismic exploration, internal multiples used to be identified as undesired noises because the conventional seismic imaging algorithms deal correctly only with primary reflections. One reason for its negative feedbacks is most of migration and inversion methods are based on the Born approximation, i.e., the assumption of one single scattering. By analyzing the role that primaries and multiples play in migration, recent studies indicate that, for a smooth and continuous velocity model, internal multiples will lead to an artificial, misleading, and false subsurface image (Berkhout and Verschuur, 2006; Behura et al., 2014; Zuberi and Alkhalifah, 2014; Li et al., 2016; Weglein, 2016). In practice, to enhance the image quality, internal multiples must be removed if we migrate seismic reflection in conventional way. It is worth to note that internal multiples has their unique characteristics, smaller reflection angle and longer ray-path, compared to primary events. These features of internal multiples recorded in seismic data could increase the aperture of illumination and enhance subsurface imaging and structure determination. In other words, instead of eliminating internal multiples in conventional imaging process, migration of internal multiples under appropriate imaging conditions could penetrate into earth to provide more stratigraphic information and to illuminate shadow zones where primaries cannot reach (Liu et al., 2011;

---

\*University of Calgary, CREWES Project

Malcolm et al., 2009, 2011; Slob et al., 2014), for example, sub-salt areas. To make use of these attractive features, internal multiples prediction need to be performed precisely as multicomponent acquisition developed.

Considerable progress of internal multiple prediction has been made recently. There are two distinguished ways to attenuate internal multiples from primary events. One is transforming internal multiples to be ‘surface-related’ and then eliminating them by their characteristics of the free surface. The representative approach, boundary-related/layer-related method, by recalibrating and exfoliating the top of the multiple generators in a stepwise way, was implemented in different domains, such as in poststack (CMP) data (Kellamis et al., 2002), in common-focus-point (CFP) domain (Berkhout and Verschuur, 2005; Berkhout, 2006), in inverse-data domain (Luo et al., 2007). The second, by considering internal multiples as the combination of a certain sub-events based on the inverse scattering series, is optimal to implement the internal multiple prediction without any subsurface information in an automatic way. Weglein et al. (1997) demonstrated that internal multiples can be estimated from sub-events which satisfy the lower-higher-lower criterion in the pseudo-depth or vertical traveltime domain. Many incentive research and discussions of inverse scattering series (ISS) on internal multiples prediction (IMP) have been presented serving diverse purposes. To correct the predicted amplitude of internal multiples and avoid the deterioration of the energy minimization adaptive subtraction, Zou and Weglein (2015) demonstrated an alternative version of ISS-IMP algorithm for all first order internal multiples in model of parameters varying in depth only. One of the key features to determine the capacity of the existing ISS-IMP algorithm in complex environments, is the search parameter selection which guarantees the selected combination to meet the lower-higher-lower relationship (Luo et al., 2007; Sun and Innanen, 2016b). To mitigate the artifacts of a fixed search parameter and to enhance the proximity of ISS algorithm, by reformulating ISS algorithm, Innanen (2017) demonstrated that inverse scattering-based internal multiple prediction can be performed with a non-stationary search parameter in time-related domains. Another promising line of research is to seek optimum domains in which apply to a relative stationary parameter. In particular, especially concerning artifact mitigation, implementation in  $\tau - p$  domain (Coates and Weglein, 1996) appears to have some attractive features (Sun and Innanen, 2015) and motivates a numerical analysis of 2D ISS internal multiple prediction in couple plane-wave domain which has a range of attractive features, practical and computational (Sun and Innanen, 2016c). Moreover, the multidimensional plane-wave-domain ISS algorithm can also be merged with non-stationary parameter to perform 2D/3D application with time-varying parameter in challenging environments.

Nevertheless, these approaches, even though powerful, are on the strength of acoustic assumption which is not reality and consistent with rapidly developed multicomponent acquisition. For inverse scattering-based approach, unlike acoustic cases, wave-mode conversion in multicomponent seismic record will wreck the wavenumber / slowness - dependent relationship of subevents in the combination and misleads the lower-higher-lower criteria. To adapt for multicomponent seismic records, by considering an isotropic-elastic-homogeneous background and decomposing the elastic inverse scattering series into types of wave-mode, Sun and Innanen (2016a) extend the elastic internal multiple prediction algorithm into 3D based on inverse scattering series, first introduced by Matson (1997), while involving wave-mode conversion.

However, preparing input for the multicomponent prediction algorithm, either proposed in pseudo-depth domain/horizontal slowness pseudo-depth domain, or plane wave domain, without causing suspicious noises and breaking lower-higher-lower relationship, is a key feature and remains to be an obstacle. Since the elastic inverse scattering series internal multiple algorithm only handles the wave-model conversion in the top layer, the reflections generated by same interface will be mislead and create aliasing combinations satisfying lower-higher-lower relationship. In this paper, details of existed issues in elastic internal multiple prediction are revealed and discussed. By computing ray-path analytically, we illustrate and compare a few different methods to prepare the inputs for multicomponent prediction including elastic stolt migration, vertical traveltime stretching, best-fitting velocity obtained by hyperbolic radon transform. A analytical comparison will also be made to discuss the advantages and shortcomings of each approach.

### ELASTIC ISS-IMP ALGORITHM

Multicomponent internal multiples prediction algorithm based on inverse scattering series was first mentioned by Matson (1997) in wavenumber-pseudo depth domain with its 2D formulation. The algorithm can be successfully extended to a full 3D case by incorporating wavenumbers with respect to two different lateral coordinates of sources and receivers in a same manner (Sun and Innanen, 2016d). The formula of the leading order multicomponent internal multiples prediction in a wavenumber pseudo-depth domain can be delineated as,

$$\begin{aligned}
 & b_3^{ij}(k_{x_g}^i, k_{y_g}^i, k_{x_s}^j, k_{y_s}^j, \omega) \\
 &= -\frac{1}{(2\pi)^4} \iiint_{-\infty}^{+\infty} dk_{x_1}^k dk_{y_1}^k dk_{x_2}^l dk_{y_2}^l e^{i\nu_1^k(z_s-z_g)} e^{-i\nu_2^l(z_s-z_g)} \\
 &\quad \times \int_{-\infty}^{+\infty} dz_1 e^{i(\nu_1^k+\nu_1^i)z_1} b_1^{ik}(k_{x_g}^i, k_{y_g}^i, k_{x_1}^k, k_{y_1}^k, z_1) \\
 &\quad \times \int_{-\infty}^{z_1-\epsilon} dz_2 e^{-i(\nu_2^l+\nu_1^k)z_2} b_1^{kl}(k_{x_1}^k, k_{y_1}^k, k_{x_2}^l, k_{y_2}^l, z_2) \\
 &\quad \times \int_{z_2+\epsilon}^{+\infty} dz_3 e^{i(\nu_2^l+\nu_2^j)z_3} b_1^{lj}(k_{x_2}^l, k_{y_2}^l, k_{x_s}^j, k_{y_s}^j, z_3)
 \end{aligned} \tag{1}$$

with,

$$\nu_M^I = \sqrt{\frac{\omega^2}{(c_0^I)^2} - (k_{x_M}^I)^2 - (k_{y_M}^I)^2} \tag{2}$$

where,  $z$  is the pseudo-depth (depth in the reference medium), and  $z_1, z_2, z_3$  satisfy the lower-higher-lower relationship, i.e.,  $z_1 > z_2$  and  $z_2 < z_3$ .  $k_{x_M}^I$  and  $k_{y_M}^I$  are  $x$  and  $y$  components of wavenumber,  $\nu_M^I$  is the vertical component of wavenumber. The subscript  $M \in \{g, s, 1, 2\}$  means the source or receiver side for a specified ray-path, i.e.,  $k_{x_M}^I$  is the  $x$  component of wavenumber corresponding to location  $(x_M, y_M, z_M)$ .  $c_0^I$  is the velocity depending on the wave mode  $I$ , and  $I = (i, j, k, l) \in \{P, SH, SV\}$ . The input  $b_1^{ij}$  is a mode-decomposed and weighted version of seismic data related:

$$b_1^{ij}(k_{x_g}^i, k_{y_g}^i, k_{x_s}^j, k_{y_s}^j, z) = -i\nu_s^j D^{ij}(k_{x_g}^i, k_{y_g}^i, k_{x_s}^j, k_{y_s}^j, z) \tag{3}$$

where,  $D^{ij}(k_{x_g}^i, k_{y_g}^i, k_{x_s}^j, k_{y_s}^j, z)$  are data associated with downgoing  $j$ -mode and upgoing  $i$ -mode with  $i, j \in \{P, SH, SV\}$ , mapped to pseudo-depth.

The prediction using equation 1 requires that all events of the inputs were sorted into the corresponded and appropriate pseudo-depth because the same pseudo-depth is utilized in all wave-types inputs. Specifically, all reflections generated by the same reflector must be mapped into the same pseudo-depth no matter what wave-mode conversions are. To keep the data-driven property of the inverse scattering series prediction algorithm, Matson and Weglein (1996) mentioned that  $D^{ij}(k_{x_g}^i, k_{y_g}^i, k_{x_s}^j, k_{y_s}^j, z)$  can be obtained using an elastic stolt migration with respect to decomposed components of shot profiles. However, no application was performed to at that moment. In this paper, we perform an elastic stolt migration in prospective of wavenumber to achieve the inputs for wavenumber pseudo-depth domain prediction.

To benefits from the constancy characteristics of the size of subevents across horizontal slowness spectrum, equation 1 can also be transferred into horizontal-slowness pseudo-depth domain and multidimensional plane wave domain in a similar way of acoustic cases (Sun and Innanen, 2017a). For  $(p, z)$  domain multicomponent prediction algorithm, it can be simply obtained by switching the wavenumber into horizontal slowness, delineated as,

$$\begin{aligned}
& b_3^{ij}(p_{x_g}^i, p_{y_g}^i, p_{x_s}^j, p_{y_s}^j, \omega) \\
&= -\frac{1}{(2\pi)^4} \iiint_{-\infty}^{+\infty} dp_{x_1}^k dp_{y_1}^k dp_{x_2}^l dp_{y_2}^l e^{iq_1^k(z_s-z_g)} e^{-iq_2^l(z_s-z_g)} \\
&\quad \times \int_{-\infty}^{+\infty} dz_1 e^{i(q_1^k+q_1^l)z_1} b_1^{ik}(p_{x_g}^i, p_{y_g}^i, p_{x_1}^k, p_{y_1}^k, z_1) \\
&\quad \times \int_{-\infty}^{z_1-\epsilon} dz_2 e^{-i(q_2^l+q_1^k)z_2} b_1^{kl}(p_{x_1}^k, p_{y_1}^k, p_{x_2}^l, p_{y_2}^l, z_2) \\
&\quad \times \int_{z_2+\epsilon}^{+\infty} dz_3 e^{i(q_2^l+q_2^j)z_3} b_1^{lj}(p_{x_2}^l, p_{y_2}^l, p_{x_s}^j, p_{y_s}^j, z_3)
\end{aligned} \tag{4}$$

with,

$$q_M^I = \sqrt{\frac{1}{(c_0^I)^2} - (p_{x_M}^I)^2 - (p_{y_M}^I)^2} \tag{5}$$

where, the input  $b_1^{ij}(p_{x_g}^i, p_{y_g}^i, p_{x_s}^j, p_{y_s}^j, z) = -iq_s^j D^{ij}(p_{x_g}^i, p_{y_g}^i, p_{x_s}^j, p_{y_s}^j, z)$ . Here,  $q$  is the corresponded vertical slowness.  $D^{ij}(p_{x_g}^i, p_{y_g}^i, p_{x_s}^j, p_{y_s}^j, z)$  can be obtained similarly by rearranging data into horizontal slowness instead of wavenumber, or by performing an elastic stolt migration in perspective of horizontal slowness.

In acoustic cases, the implementation of internal multiple prediction in plane wave domain has some advantages (Sun and Innanen, 2016c), such as the constancy distribution of each subevent in input data, allows a relative constant search parameter, fast computation. The multicomponent internal multiple prediction can also be benefited from the plane

wave domain implementation. The multicomponent internal multiple prediction in multidimensional plane wave domain can be achieved from  $(p, z)$  domain formulation using the one-to-one mapping between pseudo-depth and vertical travel time. The mathematical form is,

$$\begin{aligned}
 & b_3^{ij}(p_{x_g}^i, p_{y_g}^i, p_{x_s}^j, p_{y_s}^j, \omega) \\
 &= -\frac{1}{(2\pi)^4} \iiint\limits_{-\infty}^{+\infty} dp_{x_1}^k dp_{y_1}^k dp_{x_2}^l dp_{y_2}^l e^{i\omega(\tau_{1s}^k - \tau_{1g}^k)} e^{-i\omega(\tau_{2s}^l - \tau_{2g}^l)} \\
 &\quad \times \int_{-\infty}^{+\infty} d\tau_1 e^{i\omega\tau_1} b_1^{ik}(p_{x_g}^i, p_{y_g}^i, p_{x_1}^k, p_{y_1}^k, \tau_1) \\
 &\quad \times \int_{-\infty}^{\tau_1 - \epsilon} d\tau_2 e^{-i\omega\tau_2} b_1^{kl}(p_{x_1}^k, p_{y_1}^k, p_{x_2}^l, p_{y_2}^l, \tau_2) \\
 &\quad \times \int_{\tau + \epsilon}^{+\infty} d\tau_3 e^{i\omega\tau_3} b_1^{lj}(p_{x_2}^l, p_{y_2}^l, p_{x_s}^j, p_{y_s}^j, \tau_3)
 \end{aligned} \tag{6}$$

where, the input  $b_1^{ij}(p_{x_g}^i, p_{y_g}^i, p_{x_s}^j, p_{y_s}^j, \tau) = -iq_s^j D^{ij}(p_{x_g}^i, p_{y_g}^i, p_{x_s}^j, p_{y_s}^j, \tau)$ . Here,  $q$  is the corresponded vertical slowness, and  $D^{ij}(p_{x_g}^i, p_{y_g}^i, p_{x_s}^j, p_{y_s}^j, \tau)$  is the shot gather with the adapted  $\tau - p$  transformation related to five-coordinate: two lateral source coordinates  $(x_s, y_s) \rightarrow (p_{x_s}, p_{y_s})$ , two lateral receiver coordinates  $(x_g, y_g) \rightarrow (p_{x_g}, p_{y_g})$ , and intercept time  $t \rightarrow \tau$ .

Equation 6 requires the vertical travel time of P-P and P-SV waves are sorted into same manner, i.e.,  $\dot{P}\dot{P}$ ,  $\dot{P}\dot{S}$ , and  $\dot{S}\dot{S}$  have the same vertical traveltimes. This can be done by stretching traditional  $\tau - p$  transformed data in time dimension with appropriate factors. The input preparation for equation 1, 4, and 6 require the interpolation procedure which may increase the risk of generating aliasing.

## ELASTIC MONOTONICITY CONDITION OF PSEUDO-DEPTH/VERTICAL-TRAVELTIME AND ACTUAL DEPTH

The criteria of inverse scattering series in internal multiple prediction is to combine those events which in lower-higher-lower relationship of actual reflector depth in specified wavenumber/horizontal slowness. Therefore, the monotonic projection of pseudo-depth/vertical travel time and actual depth is essential requirement both for equation 1, equation 4, and equation 6. In this section, we will discuss the input preparation for three-different domain prediction  $(k - z, p - z, p - \tau)$  using elastic stolt-migration, time-stretching method, and best-fitting velocity model generated by high resolution hyperbolic radon transform.

### Elastic stolt migration

Matson (1997) indicated that the elastic slot migration with two constant background velocity may be utilized to preparing the input for pseudo-depth domain algorithm. However, this approach has never been examined. To perform it on shot gather, we need a prestack stolt migration scheme, which can be accomplished by stolt change (regridding) of variables in Fourier domain and followed by inverse transformation Stolt (1978). And the elastic prestack stolt migration of two component data (P- and SV-) was presented by

Etgen (1988). The image of P-P and P-SV components can be written as,

$$R_{PP}(k_m, z) = \int dk_h \int dk_{zP} \left| \frac{d\omega}{dk_{zP}} \right| P(k_m, k_h, w(k_{zP})) e^{ik_{zP}z} \quad (7a)$$

$$R_{PSV}(k_m, z) = \int dk_h \int dk_{zSV} \left| \frac{d\omega}{dk_{zSV}} \right| P(k_m, k_h, w(k_{zSV})) e^{ik_{zSV}z} \quad (7b)$$

where,  $k_{zP}$  is the dispersion relation for upcoming P waves due to a P wave source, written as

$$k_{zP} = \frac{\omega}{\alpha} \left( \sqrt{1 - \frac{\alpha^2 k_s^2}{\omega^2}} + \sqrt{1 - \frac{\alpha^2 k_g^2}{\omega^2}} \right) \quad (8)$$

$k_{zSV}$  is the dispersion relation for upcoming SV waves due to a P wave source, written as

$$k_{zSV} = \frac{\omega}{\alpha} \sqrt{1 - \frac{\alpha^2 k_s^2}{\omega^2}} + \frac{\omega}{\beta} \sqrt{1 - \frac{\beta^2 k_g^2}{\omega^2}} \quad (9)$$

and  $k_m, k_h$  are the wavenumbers related to mid-point and offset;  $k_s, k_g$  are wavenumbers related to source and receiver coordinates. The relations between them can be described by the following formula,

$$k_s = \frac{k_m - k_h}{2} \quad (10a)$$

$$k_g = \frac{k_m + k_h}{2} \quad (10b)$$

After the Fourier transformation, the first step we need is a regridding of the  $\omega$  axis to the  $k_z$  axis, which usually be performed by the interpolation of known grid values. The regridding requires the evaluation of  $\omega$  as a function of  $k_z$ . For P-P stolt migration,  $\omega(k_z)$  is given by van Trier (1948), written as,

$$\omega(k_m, k_h, k_{zP}) = \frac{\alpha k_z}{2} \sqrt{\left(1 + \frac{(k_s + g)^2}{k_z^2}\right) \left(1 + \frac{(k_g - k_s)^2}{k_z^2}\right)} \quad (11)$$

For P-SV stolt migration,  $\omega(k_z)$  is introduced by Etgen (1988), and its formulation is delineated as,

$$\omega(k_m, k_h, k_{zSV}) = \sqrt{\frac{Ak_z^2 + B(k_s^2 - k_g^2) - 2\alpha^2\beta^2 \sqrt{\alpha^2\beta^2 k_z^4 + k_z^2(k_s^2(\alpha^2\beta^2 - \alpha^4) + k_g^2(\alpha^2\beta^2 - \beta^4))}}{\beta^4 - 2\alpha^2\beta^2 + \alpha^4}} \quad (12)$$

with

$$A = \alpha^4\beta^2 + \beta^4\alpha^2; B = \alpha^2\beta^4 - \alpha^4\beta^2$$

The analytical solution of Jacobian expression  $\left| \frac{d\omega}{dk_z} \right|$  can be solved using equations 11 and 12. For P-P migration,

$$\left| \frac{d\omega}{dk_z} \right| = -\frac{\pi^2}{\Lambda(k_m, k_h, k_z)} \sqrt{\left(1 + \frac{k_m^2}{k_z^2}\right) \left(1 + \frac{k_h^2}{k_z^2}\right)} \quad (13)$$

where,

$$\Lambda(k_m, k_h, k_z) = -\frac{2\pi^2 (k_z^2 + k_h^2)(k_z^2 + k_m^2)}{\alpha (k_z^4 - k_m^2 k_h^2)}$$

For P-SV migration, it is the absolute value of the following expression,

$$\frac{d\omega}{dk_z} = \frac{1}{2(\beta^4 - 2\alpha^2\beta^2 + \alpha^4)\omega(k_z)} \times \left[ 2k_z(\alpha^4\beta^2 + \alpha^2\beta^4) - \alpha^2\beta^2 \frac{4\alpha^2\beta^2 k_z^3 + 2k_z(k_s^2(\alpha^2\beta^2 - \alpha^4) + k_g^2(\alpha^2\beta^2 - \beta^4))}{\sqrt{\alpha^2\beta^2 k_z^4 + k_z^2(k_s^2(\alpha^2\beta^2 - \alpha^4) + k_g^2(\alpha^2\beta^2 - \beta^4))}} \right] \quad (14)$$

Using equation 7, the image of P-P and P-SV reflections in a variant velocity medium can be computed by performing the elastic stolt migration with a constant velocity for P- and SV-waves separately. The elastic stolt migration is employed to be performed on a decomposed shot profile, to generate the input for prediction algorithm both in wavenumber pseudo-depth domain and in horizontal slowness pseudo-depth domain.

### Vertical time stretching

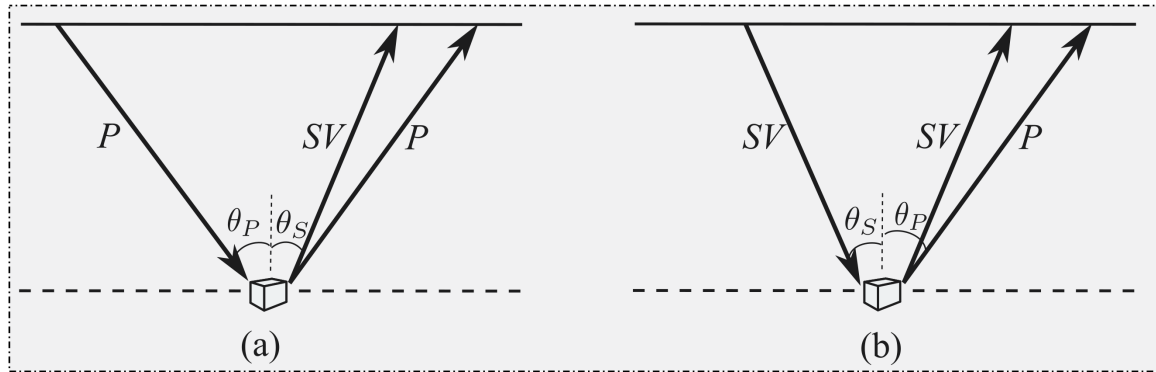


FIG. 1. Elastic waves propagating in perturbation mode in the reference medium. (a) P-wave source only, (b) S-wave source only.

For elastic plane wave prediction algorithm, due to the velocity difference between P- and SV-waves, the monotonicity condition of pseudo-depth and vertical travel time is broken. For example, Figure 1 describes ray-paths of PP-, SS-, and PS/SP-waves propagating in a reference medium through one perturbation at the same depth. However, P-P, P-SV/SV-P, and SV-SV waves have the different vertical travel time. Take a P-wave source as an example, the intercept times for PP- and PSV-waves can be calculated as,

$$\tau_{PP} = 2\tau_P = \frac{2z \cos \theta_P}{\alpha} \quad (15a)$$

$$\tau_{SP} = \tau_P + \tau_S = z \left( \frac{\cos \theta_P}{\alpha} + \frac{\cos \theta_S}{\beta} \right) \quad (15b)$$

where,  $z$  denotes the pseudo-depth in the reference medium,  $\alpha$  and  $\beta$  are the reference velocities in background, which is usually assumed to be the velocities in the top layer of

the model. Therefore, a modification needs to be made to meet the one-to-one projection of pseudo-depth and elastic vertical travel time. Considering Snell's law, the relationship between  $\tau_{PP}$  and  $\tau_{SP}$  (or  $\tau_{PS}$ ) at the same pseudo-depth can be expressed as,

$$\tau_{SP} = \tau_{PS} = \frac{\alpha + \beta}{2\beta} \tau_{PP} \quad (16)$$

Time stretching is required using equation 16 to hold the monotonic relationship between pseudo-depth and elastic vertical traveltime when the elastic internal multiple prediction is performed in multidimensional plane wave domain. In other words, the vertical travel time of input  $b_1^{SP}$  has to be stretched into the same scale of  $b_1^{PP}$ , when predicting P-P mode internal multiples; the vertical travel time of input  $b_1^{PP}$  needs to be transferred into the scale of  $b_1^{SP}$  while the prediction of P-SV mode is on. Stretching inputs in time axis also needs to interpolating the grid points using known values.

To avoid the effect of interpolation, instead of stretching the time axis of inputs, we can change the integral limits of equation 6 since the aim of time-stretching is searching combinations satisfy lower-higher-lower relationship. This leads to, keeping the simplicity of discussion, the 2D plane wave domain elastic internal multiple algorithm, which is written as,

$$\begin{aligned} b_3^{ij}(p_g, p_s, \omega) = & -\frac{1}{(2\pi)^4} \iint_{-\infty}^{+\infty} dp_1^m dp_2^n e^{i\omega(\tau_{1s}^m - \tau_{1g}^m)} e^{-i\omega(\tau_{2s}^n - \tau_{2g}^n)} \\ & \times \int_{-\infty}^{+\infty} d\tau_1^{im} e^{i\omega\tau_1^{im}} b_1^{im}(p_g^i, p_1^m, \tau_1^{im}) \int_{-\infty}^{\Upsilon(\tau_1^{im}|\tau_2^{mn})-\epsilon} d\tau_2^{mn} e^{-i\omega\tau_2^{mn}} b_1^{mn}(p_1^m, p_2^n, \tau_2^{mn}) \\ & \times \int_{\Upsilon(\tau_2^{mn}|\tau_3^{nj})}^{+\infty} d\tau_3^{nj} e^{i\omega\tau_3^{nj}} b_1^{nj}(p_2^n, p_s^j, \tau_3^{nj}) \end{aligned} \quad (17)$$

with

$$\Upsilon(\tau_2^{mn}|\tau_1^{nj}) = \begin{cases} \tau_2^{mn}, & j = m; \\ \frac{\alpha + \beta}{2\beta} \tau_2^{mn}, & j = S \ \& \ m = P; \\ \frac{2\beta}{\alpha + \beta} \tau_2^{mn}, & j = P \ \& \ m = S; \end{cases} \quad (18)$$

Note, we recommend performing the elastic internal multiple prediction with modified integral limits to hold the lower-higher-lower criteria shown as equation 17. However, to compare with the input generated by elastic stolt migration, we also created time-stretched input data in the next section.

### Pseudo-depth with best-fitting velocity

One of the major problem in elastic input preparation is how to handle the conversion of P- and SV-waves in lower layers while satisfying the lower-higher-lower relationship. However, both the elastic stolt migration with a constant velocity and time stretching method assume only one wave-mode conversion happened at the reflection point. Due to the elastic-isotropic-homogeneous background assumption, all wave-mode conversions at transmission points are neglected.

For example, in Figure 2, we have four primary events reflected by the second interface in P-component of shot profile, i.e.,  $\hat{P}\hat{P}\hat{P}\hat{P}$ ,  $\hat{P}\hat{S}\hat{P}\hat{P}$ ,  $\hat{P}\hat{P}\hat{S}\hat{P}$ ,  $\hat{P}\hat{S}\hat{S}\hat{P}$ ; another four primary events reflected by the same reflector received in SV-mode, i.e.,  $\hat{P}\hat{P}\hat{P}\hat{S}$ ,  $\hat{P}\hat{S}\hat{P}\hat{S}$ ,  $\hat{P}\hat{P}\hat{S}\hat{S}$ ,  $\hat{P}\hat{S}\hat{S}\hat{S}$ .

In the scheme of elastic stolt migration and time stretching method, these eight primary events both in P-P and P-SV components are treated as separated sub-events and will be migrated into different depths as long as they have variant pseudo-depths.  $\hat{P}\hat{P}\hat{P}\hat{P}$  and  $\hat{P}\hat{S}\hat{P}\hat{S}/\hat{P}\hat{P}\hat{S}\hat{S}$  are migrated into a similar depth with elastic stolt-migration and time-stretching because of the approximate  $v_p/v_s$  ratio in layers. Other primary events will be migrated into different depths.

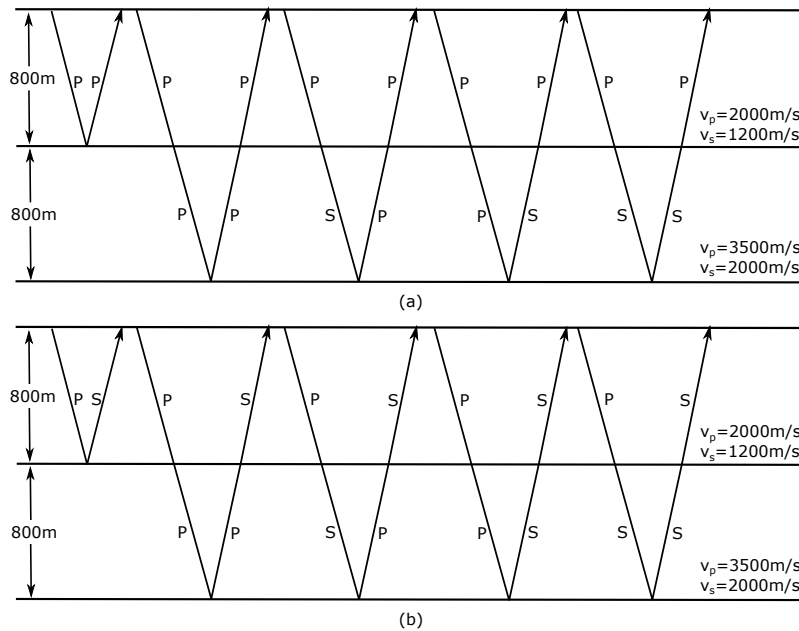


FIG. 2. Ray paths of all primary events in multicomponent reflected by the two interfaces. (a) P-P component. (b) P-SV component.

The solution of this issue is to find a special velocity related to each sub-event in the input space, which requires sub-events of inputs are separate from each other. The interval velocity is the perfect solution to this, however, it cripples the data-driven superiority of inverse scattering series prediction algorithm. Besides, it's difficult to obtain the exact velocity model and applied them to each event. The next best option for this issue is that how to find an approximate velocity for each sub-event? As we known, each sub-event in offset-time domain has a specified velocity  $v_s$ , which is the velocity parameter defines the best fit hyperbola to the actual data traveltime curve, written as

$$t^2 = t_0^2 + \frac{x^2}{v_s^2} \tag{19}$$

Therefore, the "best fit" velocity is kind of searching parameter which depends on the maximum offset in the analysis. And in variant cases, the best-fit velocity has different meanings.  $v_s$  equals to the  $v_{rms}$  (root-mean-square velocity) if the model is layered;  $v_s$

represents the stacking velocity for dipping reflector beneath a constant velocity overburden. Take the 1.5D case as example, the sub-events of input for prediction algorithm are sorted in horizontal slowness, and are separated completely in vertical traveltimes without any overlapping. Namely, a unique velocity can be obtained for each sub-event of the input as long as we have the appointed velocity for each hyperbola in offset-time domain.

Hyperbolic radon transform, a widely used technique, is the process of remapping a hyperbola curve into a single point located at its vertex. The traditional way for hyperbola transform is reconstruct the data in radon space with offset-time domain data and given a range of velocity. Its mathematical form is written as,

$$m(\tau, v) = \int_{h_{min}}^{h_{max}} d(t = \sqrt{\tau^2 + h^2/v^2}, h) dh \quad (20)$$

where,  $h$  indicates offset, and  $\tau$  is the two-way zero-offset travel time.  $v$  is the best fit velocity for the hyperbola curve.  $d(t, h)$  is the data in offset-time domain.  $m(\tau, v)$  is mapping data in radon space. With appropriate discretion and rearrangement, equation 20 can be rewritten into the matrix form as

$$\mathbf{d} = \mathbf{L}\mathbf{m} \quad (21)$$

The traditional way to reconstruct the radon panel  $m$  from equation 21 is using the transpose or adjoint operator  $\mathbf{L}^T$ . The retrieve data in radon space is given by

$$\mathbf{m} = \mathbf{L}^T \mathbf{d} \quad (22)$$

It's clear to say that transformation in equation 22 is not the inverse process of mapping using equation 21 since  $\mathbf{L}$  is not a unitary operator. Amplitudes of reconstructed traces from radon space using equation 21 are different with the original data, which could damage either the amplitude analysis or multiple prediction, if the radon panel was obtained using the adjoint operator in equation 22. Thorson and Claerbout (1985) proposed a high resolution time domain radon transform in inversion scheme using stochastic technique. Since then, the inversion scheme radon transform, both in time, frequency, and time-frequency domain, has been introduced and applied in practical seismic processing, such as multiple attenuation, offset-time space data reconstruction (Sacchi and Ulrych, 1995; Trad et al., 2002, 2003).

In the procedure of inversion, radon panel is treated as the model space,  $\mathbf{L}$  is the forward operator to reconstruct the data in offset-time domain using "model" parameter. A widely-used method to solve the sparse inversion is the least square method. The cost function for least square problem is written as,

$$J = \|\mathbf{W}_d(\mathbf{L}\mathbf{m} - \mathbf{d})\|^2 + \|\mathbf{W}_m\mathbf{m}\|^2 \quad (23)$$

where,  $\mathbf{W}_d$  is a matrix of data weights, often a diagonal matrix containing the inverse standard deviation of the data.  $\mathbf{W}_m$  is a matrix of model weights to enhance one's preference of the model, for example, sparseness or smoothness. The model weight matrix is essential to

resolve a sparse model, which is utilized to penalize large elements contained in the model space. The chosen of model weight for high resolution radon transform is well illustrated in the paper by Trad et al. (2003). We will not go into details in this paper.

A left preconditioning conjugate gradient method is employed to solve the cost function in equation 23. The full-procedure of high-resolution radon transform is solved by Re-weighted Least Square with Conjugate Gradient (RLSCG) performed as two iteration loops, external iteration and internal iteration. The external iteration is to update the model weight. The internal iteration is to solve the sparse model with current model weights by conjugate gradient.

After obtained the radon panel using hyperbolic transform, the best-fit velocity for each hyperbola can be achieved at the velocity-axis for corresponded "bright spot". The retrieve velocity model needs to be transferred into input space of prediction algorithm. Here, take the 1.5D case as an example, the input of the prediction for a single shot gather is the weighted data in linear radon space. Therefore, the velocity model retrieved from the hyperbolic radon space can be transferred into the linear radon space using elliptical radon transform, shown as,

$$\hat{d}(\tau, p) = \int_{v_{min}}^{v_{max}} m(\tau_0 = \frac{\tau}{\sqrt{1 - p^2 v^2}}, v) dv \quad (24)$$

where,  $p$  is the horizontal slowness;  $\tau$  is the vertical travel time, i.e., time axis in linear radon space;  $\tau_0$  is the two-way zero-offset travel time, i.e., time axis in hyperbola radon space;  $v$  is the best-fit velocity for hyperbola events. Then, the pseudo-depth can be obtained by velocity model multiplying with vertical travel time in linear radon space, i.e.,  $z = v\tau/2$ .

## DISCUSSION

To examine approaches described previously, in this section, we will compute the analytical solution using each method with the model illustrated in Figure 2. The pseudo-depth of stolt migration in acoustic cases is calculated by multiplying the constant background velocity with one-way vertical travelttime i.e.,  $z_s = v_0\tau/2$ , which has been verified in the paper (Sun and Innanen, 2017b). For elastic cases, it is apparent that the pseudo-depth by stolt migration is equivalent to one-way stretching-vertical time with the constant background velocity. Therefore, we will only compare the pseudo-depth of time-stretching method and the best-fitting velocity by hyperbolic radon transform. Using model parameters illustrated in Figure 2, we analytically modeled the ray-path of each event (hyperbola curves) and computed the corresponded best-fitting velocity (Table 1). Then, both of hyperbola curves and best-fit velocity was transferred into linear radon space using linear and elliptical radon transform separately, shown in Figure 3a.

Figure 3a indicates that the mapping best-fit velocity is well matched with the all sub-events in linear radon space except at the large value of horizontal slowness. These little mismatch at large value of  $p$  can be ignored and will not damages the following process in prediction because the amplitudes of sub-events at large  $p$  value in input for practical data are close to zero.

Ray-path in P-P model	Best-fitting velocity $v_s$ (m/s)
$\overset{\cdot}{P}\overset{\cdot}{P}$	2000
$\overset{\cdot}{P}\overset{\cdot}{P}\overset{\cdot}{P}\overset{\cdot}{P}$	2646
$\overset{\cdot}{P}\overset{\cdot}{P}\overset{\cdot}{S}\overset{\cdot}{P}/\overset{\cdot}{P}\overset{\cdot}{S}\overset{\cdot}{P}\overset{\cdot}{P}$	2306
$\overset{\cdot}{P}\overset{\cdot}{S}\overset{\cdot}{S}\overset{\cdot}{P}$	2000
<hr/>	
Ray-path in P-SV model	Best-fitting velocity $v_s$ (m/s)
$\overset{\cdot}{P}\overset{\cdot}{S}$	1549
$\overset{\cdot}{P}\overset{\cdot}{P}\overset{\cdot}{P}\overset{\cdot}{S}$	2314
$\overset{\cdot}{P}\overset{\cdot}{P}\overset{\cdot}{S}\overset{\cdot}{S}/\overset{\cdot}{P}\overset{\cdot}{S}\overset{\cdot}{P}\overset{\cdot}{S}$	2026
$\overset{\cdot}{P}\overset{\cdot}{S}\overset{\cdot}{S}\overset{\cdot}{S}$	1756

Table 1. The best fitting velocity for each ray-path.

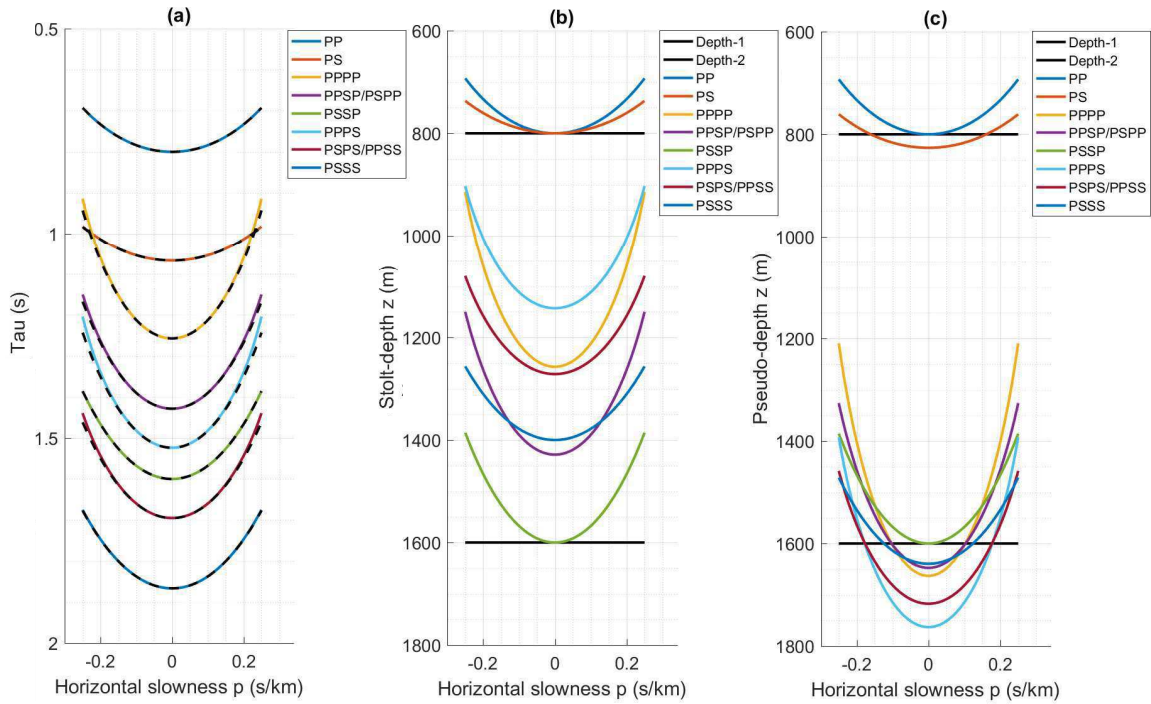


FIG. 3. Comparison between time-stretching and pseudo-depth with best-fitting velocity. (a) solid line: all ray-path in linear radon space; dot line: mapping best-fitting velocity into linear radon space using equation 24. (b) pseudo-depth obtained by multiplying a constant velocity (depend on wave-mode) multiplying with one-way vertical travel time, i.e.,  $z_s = v_0\tau/2$ . (c) pseudo-depth computed by multiplying the best-fitting velocity with one-way vertical travel time, i.e.,  $z = v\tau/2$ .

In figure 3b, two solid black lines denote the actual depth of two interfaces; the pseudo-depth is computed by constant velocity (depend on wave-mode) multiplying with one-way vertical travel time. It is clear that two primary events reflected by the 1st interface are matched precisely at  $p = 0$  and the mismatch increases as the growing of horizontal slowness. However, those primary events reflected by the 2nd reflector, which should be migrated at the same pseudo-depth, have a very large gap either at small or at large value of horizontal slowness. These errors of pseudo-depth can misleads the lower-higher-lower relationship when the selected search parameter is smaller than them. This is also the reason

we implemented multicomponent internal multiple prediction with very aggressive integral limits in the report of last year. And the pseudo-depth with time-stretching method is equivalent to the pseudo-depth migrated by elastic slot migration with a constant background velocity, which will be testified later in the application section.

Using the best-fitting velocity illustrated in Table 1, we also calculated the pseudo-depth by multiplying them with one-way vertical traveltimes (Figure 3a). The result is shown in Figure 3c. With the estimated unique velocity, the pseudo-depth of primary reflected by 1st reflector has a small constant gap as the horizontal slowness increasing. For those primaries reflected by the 2nd interfaces, the largest gap was located at  $p = 0$ , but is much smaller compared to the pseudo-depth obtained by the constant velocity. In this case, the largest gap in pseudo-depth using best-fitting velocity is around 150m, which equals to 37 grid sizes if we have 4ms for time interval. It leads to a relative larger search parameter to treat all those reflections as a single sub-event and to avoid the false lower-higher-lower relationship during selecting combination.

Based on this, we may conclude that, comparing to elastic stolt-migration and time-stretching method, the internal multiple prediction with the best-fitting velocity model may have a better solution to monotonicity condition for identifying lower-higher-lower relationship, but still cannot handle the short-leg internal multiples, i.e., generated by thin layers. It seems like that the advantage of plane-wave prediction algorithm in allowing a small relative stationary search parameter is weakened by the best-fitting velocity model. To solve this, a detail needs to be noted that most of these primary events generated by 2nd interface are sorted in an opposite (ascending or descending) order in Figure 3b and 3c. Therefore, we can make use of this property to filter the combination selected using best-fitting velocity model, i.e., only combinations satisfy the intersection of time-stretching and best-fitting velocity in lower-higher-lower relationship will be selected to reconstruct internal multiples. The intersected comparison in pseudo-depth will allow us to select a common-wide search parameter, i.e.,  $\epsilon$  in grid points is the width of source wavelet, in the implementation of plane-wave domain internal multiple prediction. In Part II, we will use a simple synthetic application to verify and examine the comparisons and conclusions we summarized previously.

## CONCLUSION

The wave-model conversion in multicomponent data is a hazard of input preparation for inverse scattering series internal multiple prediction, which misleads the lower-higher-lower relationship of sub-events. To better understand the mechanism of each approach for multicomponent input preparation, we modeled ray-path of each primary sub-event and computed the corresponded pseudo-depth analytically using elastic stolt-migration, vertical traveltimes stretching method, and best-fitting velocity model generated by high-resolution hyperbolic radon transform. Analytical comparison indicated that, theoretically, elastic stolt migration sorted the input in pseudo-depth as the vertical traveltimes stretching method does. Both of them can migrate events by first interfaces from multicomponent shot profile into the same pseudo-depth as expected. However, events reflected by lower interfaces are failed to be shifted into the same pseudo-depth, which may produce suspicious combinations satisfying lower-higher-lower relationship. The best-fitting velocity model

gives an approximate solution for identifying lower-higher-lower relationship, which requires a large constant search parameter. However, the pseudo-depth of those events using time-stretching and best-fitting velocity are sorted in an opposite order. Taking advantage of that, the cross-validation of time-stretching and best-fitting velocity may leads to a constant smaller search parameter.

## ACKNOWLEDGEMENTS

We thank the sponsors of CREWES for continued support. This work was funded by CREWES industrial sponsors and NSERC (Natural Science and Engineering Research Council of Canada) through the grant CRDPJ 461179-13.

## REFERENCES

- Behura, J., Wapenaar, K., and Snieder, R., 2014, Autofocus imaging: Image reconstruction based on inverse scattering theory: *Geophysics*, **79**, No. 3, A19–A26.
- Berkhout, A., 2006, Seismic processing in the inverse data space: *Geophysics*, **71**, No. 4, A29–A33.
- Berkhout, A., and Verschuur, D., 2005, Removal of internal multiples with the common-focus-point (cfp) approach: Part 1—Explanation of the theory: *Geophysics*, **70**, No. 3, V45–V60.
- Berkhout, A., and Verschuur, D., 2006, Imaging of multiple reflections: *Geophysics*, **71**, No. 4, SI209–SI220.
- Coates, R., and Weglein, A., 1996, Internal multiple attenuation using inverse scattering: Results from prestack 1 & 2d acoustic and elastic synthetics, *in* 1996 SEG Annual Meeting, Society of Exploration Geophysicists.
- Etgen, J. T., 1988, Elastic prestack migration of two component data: *Geophysics*, 289–306.
- Innanen, K. A., 2017, Time and offset domain internal multiple prediction with non-stationary parameters: *Geophysics*, accepted.
- Kelamis, P. G., Erickson, K. E., Verschuur, D. J., and Berkhout, A., 2002, Velocity-independent redatuming: A new approach to the near-surface problem in land seismic data processing: *The Leading Edge*, **21**, No. 8, 730–735.
- Li, Z., Li, Z., Wang, P., and Zhang, M., 2016, Reverse time migration of multiples based on different-order multiple separation: *Geophysics*, **82**, No. 1, S19–S29.
- Liu, Y., Chang, X., Jin, D., He, R., Sun, H., and Zheng, Y., 2011, Reverse time migration of multiples for subsalt imaging: *Geophysics*, **76**, No. 5, WB209–WB216.
- Luo, Y., Zhu, W., Kelamis, P. G. et al., 2007, Internal multiple reduction in inverse-data domain: *SEG Expanded Abstracts*. San Antonio:[sn], 125–129.
- Malcolm, A. E., De Hoop, M. V., and Ursin, B., 2011, Recursive imaging with multiply scattered waves using partial image regularization: A north sea case study: *Geophysics*, **76**, No. 2, B33–B42.
- Malcolm, A. E., Ursin, B., and Maarten, V., 2009, Seismic imaging and illumination with internal multiples: *Geophysical Journal International*, **176**, No. 3, 847–864.
- Matson, K., and Weglein, A. B., 1996, Removal of elastic interface multiples from land and ocean bottom data using inverse scattering, *in* SEG Technical Program Expanded Abstracts 1996, Society of Exploration Geophysicists, 1526–1530.
- Matson, K. H., 1997, An inverse scattering series method for attenuating elastic multiples from multicomponent land and ocean bottom seismic data: Ph.D. thesis, University of British Columbia.

- Sacchi, M. D., and Ulrych, T. J., 1995, High-resolution velocity gathers and offset space reconstruction: *Geophysics*, **60**, No. 4, 1169–1177.
- Slob, E., Wapenaar, K., Brogini, F., and Snieder, R., 2014, Seismic reflector imaging using internal multiples with marchenko-type equations: *Geophysics*, **79**, No. 2, S63–S76.
- Stolt, R., 1978, Migration by fourier transform: *Geophysics*, **43**, No. 1, 23–48.
- Sun, J., and Innanen, K. A., 2017a, Multicomponent inverse scattering series internal multiple prediction in the  $\tau$ -p domain, *in* SEG Technical Program Expanded Abstracts 2017, Society of Exploration Geophysicists, 2491–2496.
- Sun, J., and Innanen, K. A. H., 2015, 1.5 d internal multiple prediction in the plane wave domain: CSEG Geoconvention.
- Sun, J., and Innanen, K. A. H., 2016a, Implementation of predicting elastic internal multiples based on inverse scattering series: synthetic results: CREWES Research Report, **28**, 1–15.
- Sun, J., and Innanen, K. A. H., 2016b, Interbed multiple prediction on land: which technology, and which domain?: CSEG recorder, **41**, No. 8, 24–29.
- Sun, J., and Innanen, K. A. H., 2016c, Inverse-scattering series internal-multiple prediction in the double tau-p domain, *in* SEG Technical Program Expanded Abstracts 2017, Society of Exploration Geophysicists, 4555–4560.
- Sun, J., and Innanen, K. A. H., 2016d, Theoretical framework of elastic internal multiples prediction based on inverse scattering series: CREWES Research Report, **28**, 1–21.
- Sun, J., and Innanen, K. A. H., 2017b, Numerical aspects of inverse scattering series internal multiple prediction in the coupled plane wave domain: *Geophysics*, **submitted**.
- Thorson, J. R., and Claerbout, J. F., 1985, Velocity-stack and slant-stack stochastic inversion: *Geophysics*, **50**, No. 12, 2727–2741.
- Trad, D., Ulrych, T., and Sacchi, M., 2003, Latest views of the sparse radon transform: *Geophysics*, **68**, No. 1, 386–399.
- Trad, D. O., Ulrych, T. J., and Sacchi, M. D., 2002, Accurate interpolation with high-resolution time-variant radon transforms: *Geophysics*, **67**, No. 2, 644–656.
- van Trier, J., 1948, Inversion of seismic data in the fourier domain and prestack stolt migration.
- Weglein, A. B., 2016, Multiples: Signal or noise?: *Geophysics*, **81**, No. 4, V283–V302.
- Weglein, A. B., Gasparotto, F. A., Carvalho, P. M., and Stolt, R. H., 1997, An inverse-scattering series method for attenuating multiples in seismic reflection data: *Geophysics*, **62**, No. 6, 1975–1989.
- Zou, Y., and Weglein, A. B., 2015, An internal-multiple elimination algorithm for all first-order internal multiples for a 1d earth, *in* SEG Technical Program Expanded Abstracts 2015, Society of Exploration Geophysicists, 4408–4412.
- Zuberi, M. A. H., and Alkhalifah, T., 2014, Generalized internal multiple imaging: *Geophysics*, **79**, No. 5, S207–S216.